ELSEVIER

Contents lists available at ScienceDirect

## **Control Engineering Practice**

journal homepage: www.elsevier.com/locate/conengprac



# A novel integrated fuzzy control system toward automated local airflow management in data centers



Ghazal Mohsenian <sup>a,\*</sup>, Sadegh Khalili <sup>a</sup>, Mohammad Tradat <sup>a</sup>, Yaman Manaserh <sup>a</sup>, Srikanth Rangarajan <sup>a</sup>, Anuroop Desu <sup>b</sup>, Dushyant Thakur <sup>d</sup>, Kourosh Nemati <sup>c</sup>, Kanad Ghose <sup>b</sup>, Bahgat Sammakia <sup>a</sup>

- <sup>a</sup> Departments of Mechanical Engineering, ES2 Center, Binghamton University-SUNY, NY, 13902, United States of America
- <sup>b</sup> Departments of Computer Science, ES2 Center, Binghamton University-SUNY, NY 13902, United States of America
- <sup>c</sup> Future Facilities, Inc., New York, NY 10001, United States of America
- <sup>d</sup> MathWorks, Natick, MA 01760, United States of America

### ARTICLE INFO

# Keywords: Airflow management Dynamic workload Colocation data centers CRAHs' control Artificial neural network Automated data center

### ABSTRACT

Today, Data Centers (DCs) are dynamic environments with considerable fluctuations in workload and power dissipation. As a result, active monitoring and dynamic thermal management strategies are essential. In this study, an automated dynamic airflow management technique using air dampers was introduced to manage cold air delivery to individual aisles based on the Information Technology Equipment (ITE) airflow demand. Within this management system, pressure measurements inside the Cold Aisle Containment (CAC) and the plenum were considered controlled variables. First, a feedback fuzzy controller was designed to regulate the airflow delivered to the aisles by adjusting the Open Area Ratio (OAR) of the air dampers. Then, to improve the system's performance and to implement a control system which was adaptable to environmental changes, another fuzzy controller was developed to adjust the blower speed of the cooling units. To estimate the required airflow for provisioning all the ITE in a DC, an Artificial Neural Network (ANN) was developed to characterize the air dampers. This study experimentally examined several opportunities for improving the thermal management and energy performance of DCs with automatic control schemes. Experimental data showed that by using the proposed cooling control strategy, 75% of the cooling units' blower powers and 16% of the chiller's power were saved while maintaining proper thermal management conditions compared to the worst case scenario in which the air dampers were completely open and the cooling units' blower speeds were at maximum. Experimental data from the implementation of the holistic control methodology indicated that there was minimal air leakage from the plenum to the room. Additionally, this approach achieved more efficient airflow delivery from CRAH units to the cold aisles with minimal air loss through leakage.

### 1. Introduction

DCs have become an indispensable part of modern computing infrastructures. Demand for real-time data transmission is at an all-time high. As colocation (COLO) services and cloud solutions become popular among organizations, the number of DCs has grown significantly. Data centers are accounted for approximately 1% of the national electricity use (Saiyad et al., 2021). Since cooling systems consume (30–50)% of total energy consumption (Chu & Wang, 2019; Ham, 2015; Rong et al., 2016) efficient cooling strategies play a vital role in the thermal management of DCs. Different cooling techniques are used in DCs, namely air cooling, liquid cooling, immersion cooling, and two-phase cooling. However, when it comes to the most reliable, well-developed, and widespread cooling strategy, air cooling takes the lead.

In an air-cooled DC, the chilled airflow path can be identified either as a short-distance or long-distance cooling system (Chu & Wang, 2019). For short-distance cooling, airflow may circulate close to the computer racks. In-row cooler or rack mounted cooling systems are typical examples of short-distance cooling. For long-distance cooling systems, Raised Floor (RF) and overhead air supply systems may be utilized. Airflow management with these two cooling systems are discussed extensively in the literature (Athavale, Joshi, & Yoda, 2018; Khalili et al., 2018; Manaserh, Tradat, Mohsenian, Sammakia and Seymour, 2020; Nada & Said, 2017; Nada et al., 2017; Nemati, 2016; Nemati, Alissa, & Sammakia, 2015; Tradat et al., 2020; Wang, Tsui, & Wang, 2017). In a typical RF data center, the plenum is pressurized with cold air from the Computer Room Air Handler (CRAH) or

E-mail address: gmohsen1@binghamton.edu (G. Mohsenian).

<sup>\*</sup> Corresponding author.

	Nomenclature						
	ANN	Artificial Neural Network					
	ASHRAE	American Society of Heating, Refrigeration, and Air-Conditioning Engineers					
	CAC	Cold Aisle Containment					
	COLO	Colocation					
CRAC		Computer Room Air Conditioner					
CRAH		Computer Room Air Handler					
	DC	Data Center					
	ES2	Center for Energy-Smart Electronics Sys-					
		tems					
	IPMI	Intelligent Platform Management Interface					
	ITE	Information Technology Equipment					
	OAR	Open Area Ratio					
	RAT	Return Air Temperature					
	RF	Raised Floor					
	RWT	Return Water Temperature					
	SAT	Supply Air Temperature					
	SNMP	Simple Network Management Protocol					
	SWT	Supply Water Temperature					
	VFD	Variable Frequency Drive					

Computer Room Air Conditioner (CRAC). Installing perforated tiles allows cold air to be delivered to the intakes of the rack-mounted equipment. Managing the placement of the RF tiles is critical. Typically, perforated tiles are positioned in front of the ITE racks. The hot air returns to the cooling units via a ceiling plenum or open room. Many technologies improve the cooling efficiency in raised floor DCs, such as containment systems, integrated fans, and air dampers. Hot or cold aisle containment separates the supply cold air from the return hot air, which is one of the most promising energy-efficient strategies used in DCs today. Preventing the hot and cold airstreams from mixing with the help of containments promotes a uniform ITE inlet temperature profile, allows for a higher cooling unit Supply Air Temperature (SAT), eliminates hot spots, and improves power efficiency (Alissa et al., 2016a; Muralidharan et al., 2013; Shrivastava, Calder, & Ibrahim, 2012; Shrivastava & Ibrahim, 2013). Numerous research studies have been conducted on various aspects of using containments.

Most DC operators grossly over provision the aisles to prevent recirculation and the formation of hotspots. This strategy is overly conservative and inefficient. Providing adequate airflow to the ITE will maximize a DC's efficiency. Hence, introducing different control systems at the component and system level that react to the environmental changes in the DCs are potential solutions (Khalid & Wemhoff, 2019; Lucchese & Johansson, 2019; Manaserh, Tradat, Mohsenian, Sammakia and Ortega, 2020; Zheng et al., 2018). Baxendale et al. presented a temperature PI control system methodology to maintain a target server inlet air temperature by changing the CRAC Return Air Temperature (RAT) set points for more effective DC monitoring (Baxendale et al., 2019). In another study, a linear quadratic regulator controller was designed for DC cooling. Therein, using the maximum and mean inlet server temperature as feedback signals and the CRAH output temperature as a manipulated variable achieved the best cooling performance index (Garcia-Gabin, Mishchenko, & Berglund, 2018). Boucher et al. proposed three types of actuators, namely CRAC supply temperature, CRAC fan speed, and plenum vent tile openings, as control parameters to optimally distribute cooling resources in DCs (Boucher et al., 2005). Bash et al. utilized a distributed sensor network to the racks and designed a PID controller to adjust the SAT and flow rate from the CRAH according to the set point (Bash, Patel, & Sharma, 2006). Another control system for dynamic thermal management in

DCs used a multi-input-multi-output controller to adjust the adaptive vent tile openings based on rack inlet temperature (Beitelmal et al., 2009; Wang et al., 2009). A model-based predictive controller was developed to maintain the temperature of the rack below a certain threshold. Another approach to manage airflow was the deployment of active tiles that had integrated fans. Arghode et al. showed a lower and more uniform server inlet temperature using active tiles in a fully provisioned cold aisle compared to an under provisioned containment with passive tiles (Arghode, Sundaralingam, & Joshi, 2016). However, the fans in the active tiles required power, which increased operating costs. Moreover, the fans' batteries which will be used in case of power outages, blocked a large portion of the tiles' surfaces.

An alternative approach to local airflow management is using remotely controllable air dampers (Fig. 1). The electric motors in these dampers adjust the angle of the vanes only when it is needed. This reduces battery size and increases longevity. To the best of the authors' knowledge, previous studies on airflow management techniques considered different temperatures, such as the SAT from the CRAH units, RAT to the cooling units, and inlet or outlet temperature of the servers, as a controlled variable for different cooling control systems. However, using temperature as a controlled variable has a shortcoming in over provisioned aisles. At steady state conditions, the ITE inlet temperature will match the SAT of CRAH units. As a result, when cooling units provide excessive airflow inside aisles with an allowable range of temperature, the control system cannot detect over provisioning and react accordingly because the controlled variable has not changed.

This paper outlined an architecture and control scheme for dynamic thermal management of air-cooled DCs. In this study, remotely controllable air dampers were used to better match the cold air delivery to individual aisles, which was done based on the ITE airflow demand under various conditions (over provision and/or under provision). What distinguished this work from previous studies was that it considered the differential pressure between the CAC and room ( $\Delta P_{CAC-room}$ ) as well as the differential pressure between the plenum and room  $(\varDelta P_{Plenum-room})$ as the controlled variables. In a previous study, a fuzzy control system was designed to adjust the angle of the damper's vane to regulate the required cold air based on  $\Delta P_{CAC-room}$  at the rack level (Mohsenian, 2020; Mohsenian, Khalili, & Sammakia, 2019). Afterward, the controller's performance was investigated at the presence of ITE load variation at the aisle level (Khalili et al., 2019). After the controller was tested at the rack and aisle levels, and the proof of concept was illustrated, the size of the testbed was then expanded to include two aisles with 38 racks for scalability. Moreover, without any control over the blower speed of the cooling units, having a provisioned DC was challenging especially in cases where the cooling units' blower speed was excessively high or low. This paper introduced another fuzzy control system to regulate the CRAH units' blower speeds in series with the dampers' controller for the purpose of being automated, independent of the DC layout, and adaptable to changes in ITE workload. The developed control system regulated the fan speeds of cooling units' blower by adjusting the Variable Frequency Drive (VFD) based on a constant range of pressure in the plenum. Hence, a feedforward neural network was employed to represent the effect of damper openness and differential pressure across the damper on the airflow rate acquired from air dampers. ANN could be leveraged to represent nonlinear heat transfer and flow processes in a DC (Song, Murray, & Sammakia, 2013, 2014). Consequent energy saved by using the proposed holistic control technique was investigated.

### 2. Experimental setup

### 2.1. Facility description

The ES2 data center layout and the aisles configurations are illustrated in Fig. 2. All the experiments in this study were conducted at the ES2-Data Center Laboratory at the State University of New York at

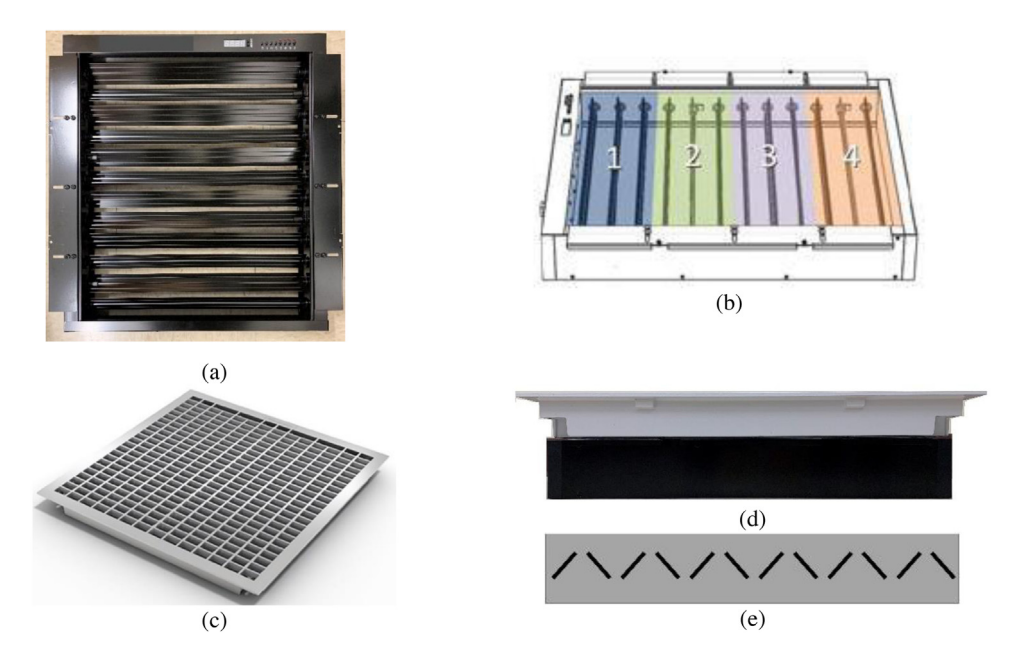


Fig. 1. Air damper. (a) Top view of air damper. (b) Different zones for airflow control. (C) Directional floor tile. (d) Side view of the damper mounted under a perforated tile. (e) Schematic of the damper's vane.

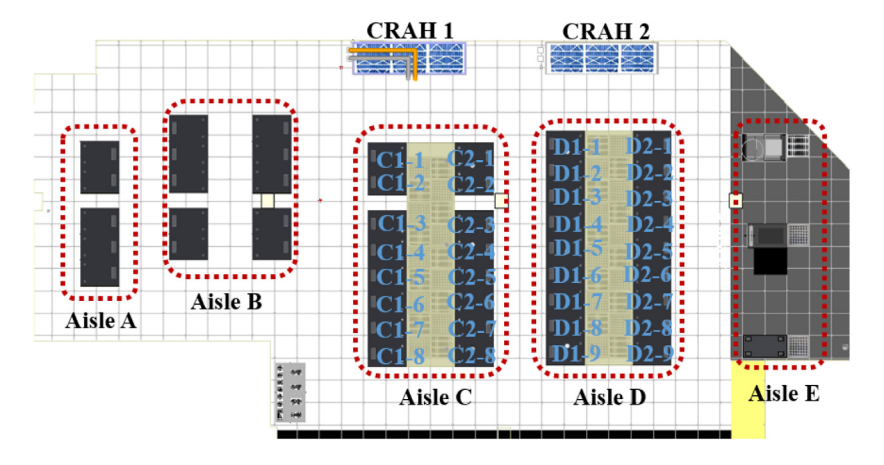


Fig. 2. Layout of the ES2 data center laboratory at Binghamton University.

Table 1
List of ITE and their airflow demand in aisles C and D.

	ITE	Required airflow rate [CFM]	Total number	Total airflow demand [CFM]
	Dell PE R530 — Conf.1	35	80	2800
	Dell PE R530 — Conf.2	37	32	1184
	Dell PE R520	33	61	2013
Aisle C	Dell PE R730	33	6	198
	HP PL DL380/385 G6	34	64	2176
	HP PL DL380/385 G7	35	13	455
	Dell PE 2950	44	3	132
	Dell PE C2100	34	14	476
	Network Switch	29	16	464
Sum			289	9898
	HP PL DL385 G2	43	36	1548
Aisle D	Dell PE 2950	44	112	4928
	Blade Center	243	12	2916
	Network Switch	29	12	348
Sum			172	9740

Binghamton. The ES2 data center had a 215 m<sup>2</sup> (2315 ft<sup>2</sup>) space with a 0.91 m (3 ft) underfloor plenum and a 5.18 m (17 ft) ceiling height. It was equipped with two chilled water based CRAH units, which were rated at 114 kW (32 tons) of cooling capacity. The vendor specified cooling units' nominal airflow rates were 16 500 CFM and 17 500 CFM for CRAH1 and CRAH2, respectively. VFD was used to modulate the supply airflow rate. The layout design for the server racks and other computing equipment was in a hot aisle/cold aisle arrangement. The DC laboratory consisted of five cold aisles (A, B, C, D, and E). This study was carried out in aisles C and D, which were fully contained. The number of tiles in aisles C and D was 18 and 20, respectively. In aisle C, a total of 289 2-RU servers were arranged in 16 racks. Aisle D contained 18 racks and 172 servers. The servers in aisles C and D were from different vendors, had different heights, and were from different generations. Table 1 shows the ITE that were installed in aisles C and D along with their corresponding design airflow demands when the  $\Delta P$ across the server is equal to zero. The environmental conditions for which the specified airflow was given were an inlet air temperature of 20 °C and a relative humidity of 45%.

### 2.2. Instrumentation

The airflow demand of each ITE was measured by mounting a server on an airflow test chamber designed in accordance with AMCA 210-99/ASHRAE 51-1999. Alissa et al. explained the procedure for obtaining an active flow curve (Alissa et al., 2016b). Differential pressure between the CAC and the laboratory airspace was measured using Bapi ZPT-LR pressure sensors with a measurement range of 0 to  $1^{\prime\prime}$ wc (0-249 Pa) and an accuracy of  $\pm 0.25\%$  of the range (0.625 Pa). Moreover, One-Touch differential pressure transmitter sensors (series 616KD) were used to report the differential pressure between the underfloor plenum and the airspace above the RF with an uncertainty of  $\pm 2\%$  of full scale in the measurements. To ensure static pressure was measured in all the cases, a pressure diffuser is used at the end of the probes inside the CAC and plenum. Perforated cardboard boxes were placed around the static pressure probes inside the plenum because the air velocity there was higher than in the CAC (Fig. 3f). A 34980 A multifunction switch/measure unit was used to collect all the pressure readings inside the CAC and the plenum. Furthermore, the servers' fan speeds and inlet temperatures were obtained by gathering the IPMI data of ITE using the Linux operating system. Finally, the volumetric flow rate of the perforated tiles was measured with a back pressure compensated airflow device, known as a flow hood (ADM-850L), as shown in Fig. 3h.

The experimental setup for different scenarios and conditions is shown in Fig. 4. During all tests, air dampers were set in single zone mode and were installed under directional tiles. Two different thermal zones (COLO layout) were specified. Aisle C with assigned CRAH 1 was defined as zone 1 and aisle D with assigned CRAH 2 was defined as zone 2 (Fig. 2). Dampers were placed in a staggered layout. Hence, aisles C and D contained 9 and 10 dampers, respectively. Six pressure sensors were installed at the top of racks C2–1, C2–4, C2–8, D1 -1, D1–5, and D1–9. Six other pressure transmitter sensors were installed in the plenum halfway up the pedestals across aisles C and D to measure the pressure distribution, as shown in Fig. 4c.

# (a) (b) (c) (c) (d) (e)



### 3. Methodology of control system for local airflow

Providing significantly more airflow than the amount required by equipment racks is known as over provisioning (1 >  $\Delta P_{\rm CAC-room}$  > 0). Many DC operators typically over provision the aisles to guarantee adequate thermal margins, which leads to significant energy loss due to cold air bypass and leakages. On the other hand, when the available cold air is less than ITE airflow demand, the aisles are under provisioned. Hot air recirculation, hot spots, and elevated ITE fans speeds are consequences of an under provisioned aisle ( $\Delta P_{\rm CAC-room}$  < 0). It is vital to provide ITE with access to adequate air (provisioned) at a proper temperature to ensure their optimal operation ( $\Delta P_{\rm CAC-room}$  = 0).

In this study, the proposed methodology used a fuzzy algorithm to control the  $\Delta P_{\rm CAC-room}$  and  $\Delta P_{\rm Plenum-room}$  in a raised floor DC. This study was conducted in a closed containment; hence, the temperature was uniform inside the CAC. This methodology addressed both over and under provisioned scenarios and detected ITE starvation. Generally, the fuzzy algorithm is suitable for control problems where constructing a precise mathematical model is difficult or expensive (Klir & Yuan, 1995). In this study, these difficulties arose from system nonlinearity, the time-varying nature of the process to be controlled, a large unpredictable environmental disturbance, and the complexity of leakage characterization through gaps in the cabinet, containment, and RF.

Fuzzy logic uses linguistic descriptions to define the relationship between the input information and the output action (Raymond, Boverie, & Titli, 1994; Simoes, 2010; Wong & Feng, 1994; Zadeh, 1973). In this study, a fuzzy controller operated by repeating a cycle of the following four steps: First, measurements were taken of all variables ( $\Delta P_{\text{CAC-room}}$  and  $\Delta P_{\text{Plenum-room}}$ ) that represent relevant conditions of the controlled process. Next, the error signals were monitored. The error signal was defined as the difference between the actual value of the controlled variables and their desired value. Based on the result of this evaluation and control rules, the fuzzy controller produced values of controlling variables that represented relevant control actions. Finally, the fuzzy

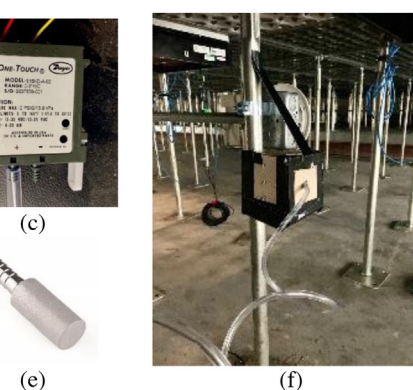




Fig. 3. Instruments. (a) Flow bench setup. (b) Bapi ZPT-LR pressure sensor. (c) One-Touch differential pressure transmitter sensor. (d) Pressure diffuser at the end of the probe inside the CAC. (e) Pressure diffuser installed in the plenum. (f) Perforated cardboard box around the pressure probe inside the plenum. (g) 34 980 A data acquisition. (h) Flow hood.

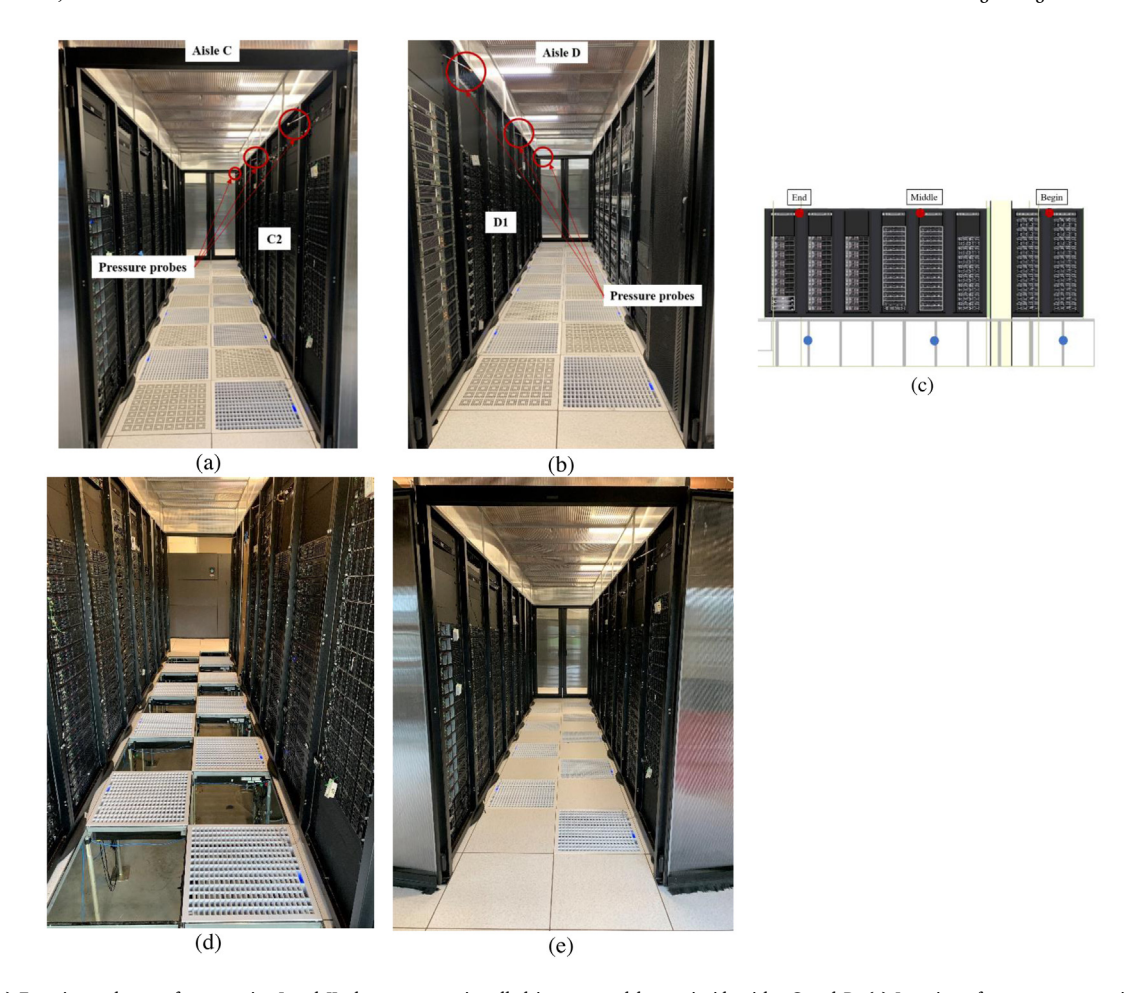


Fig. 4. (a) & (b) Experimental setup for scenarios I and II, dampers were installed in staggered layout inside aisles C and D. (c) Location of pressure sensors inside aisles C and D as well as inside the plenum at the middle of pedestals. (d) Perforated tiles were removed in aisles C and D. (e) Experimental setup for scenario III, new layout of ES2 data center with solid tiles.

controllers allowed sufficient time for the system to reach a steady state before assessing any other changes in the system.

One of the potential challenges for implementing a fuzzy controller for the dampers' OAR based on the pressure measurements for multiple aisles is the interdependency of the aisles. In a multiple aisle DC with a common RF, adjusting the dampers' OAR in one aisle will affect the air delivery, CAC pressure, and plenum pressure of the other aisles. Moreover, in a typical raised floor DC, cooling units have no control over the destination of the cold air. To have an automated DC and manage the local airflow in DCs efficiently, having control over the cooling units' blower speeds alongside dampers' openness is necessary. These two fuzzy control systems work in series and thus have an impact on each other's performance. A general scheme for these two control systems is shown in Fig. 5.

### 3.1. Control system of air dampers

The local flow rate was adjusted by controlling the angle of the dampers' vanes, which are drop-in replacements for conventional fixed-opening vent tiles. A fuzzy feedback controller was designed to adjust the dampers' OAR, to supply enough air to cool down the servers. The average differential pressure between the CAC and the room across individual aisles was used as a point of reference for evaluating the system's provisioning level. In this study, the goal was to maintain or reach a neutral provisioning state while 1 Pa of CAC over provisioning was allowed (0 Pa  $\leq$   $\Delta P_{\text{CAC-room}} = \Delta P_{\text{Ideal}} \leq$  1 Pa). The designed fuzzy controller adjusted the dampers' OAR via Simple Network Management Protocol (SNMP) with various rates. The rate of change in the dampers'

OAR depended on the error signal magnitude to prevent pressure overshooting or instability and fluctuation in the pressure near zero. If the error signal was small, then the fuzzy controller changed the dampers' OAR with a fixed small step. If the error signal was large, then the control system measured the CAC pressure response after first making an arbitrary change in the damper's OAR. Subsequently, the controller approximated the next damper's OAR using linear regression to reach full provisioning, which was based on the controller's deviation from differential pressure set points. It is worth mentioning that the controller monitored the pressure every 10 s during normal operation but slept for 40 s after each change in the dampers' OAR to allow sufficient time for the system to reach a steady state before assessing the pressure condition again. An analogy of the control strategy can be formulated as follows:

The goal is: 0 Pa  $\leq \Delta P_{Ideal} \leq 1$  Pa

$$\begin{split} 3 &< \Delta P_{CAC-room} \\ \text{IF } 2 &< \Delta P_{CAC-room} < 3 \parallel \\ -3 &< \Delta P_{CAC-room} < -1 \\ \text{IF } 1 &< \Delta P_{CAC-room} < 2 \parallel \\ -1 &< \Delta P_{CAC-room} < 0 \end{split}$$

**IF**  $\Delta P_{\text{CAC-room}} < -3$ 

THEN change the dampers' OAR by 15%, afterward use linear regression to reach  $\Delta P_{Ideal}$ . THEN change the dampers' OAR by constant rate of 10% to reach  $\Delta P_{Ideal}$ . THEN change the dampers' OAR by constant rate of 4% to reach  $\Delta P_{Ideal}$ .

### 3.2. Control system of cooling units

The default CRAH controller adjusted the chilled water valve based on the SAT set point. Therefore, the fan speed of the cooling units always stayed unchanged at maximum speed. However, the blower

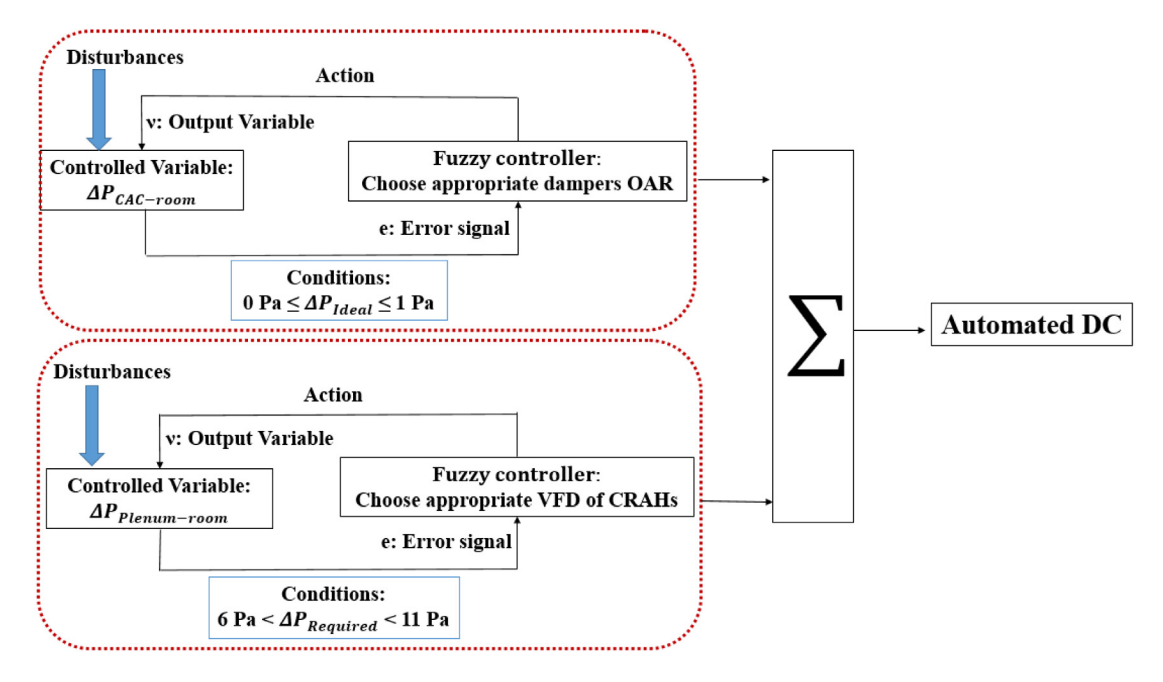


Fig. 5. Fuzzy controllers' scheme.

speeds of the CRAH units were adjusted using VFD to modulate supplied airflow rates based on the ITE demand. A fuzzy control system was designed based on maintaining a constant range of differential pressure between the plenum and room. In this study, the required range of  $\Delta P_{\rm Plenum-room} = \Delta P_{\rm Required}$  was estimated to be between 6 Pa and 11 Pa, which will be addressed in Section 3.3. To regulate the average plenum pressure, the fuzzy controller sent a signal (using SNMP commands) to the VFD to change the CRAHs' blower speeds based on the difference between the measured pressure and the required pressure range in the plenum. The controller adjusted the VFD of the CRAH units with fixed small steps in each cycle. To avoid instabilities, after each change in the CRAH units' VFD, the fuzzy control system slept for 60 s. The fuzzy controller consisted of the following rules:

The goal is: 6 Pa  $< \Delta P_{Required} < 11$  Pa

IF  $\Delta P_{Required} < 6$  THEN increase the cooling units' VFD by 5%, to reach  $\Delta P_{Required}$ .

IF  $11 < \Delta P_{Required}$  THEN decrease the cooling units' VFD by 5%, to reach  $\Delta P_{Required}$ .

### 3.3. Estimating required range of plenum pressure

To accurately estimate the required range of pressure in any DC raised floor plenum, ITE airflow demand, cold air supplied by cooling units, and plenum leaks must be determined. The lower range of pressure in the plenum was specified based on the airflow demand and the number of dampers in each aisle. Furthermore, understanding the interaction between aisles and leakages in the RF was necessary to specify the upper range of pressure in the plenum. The following approach was used to specify the lower and upper bound for the desired plenum pressure: The flow bench was used to obtain flow rate data for different OAR and  $\Delta P$  across the dampers. Fig. 6a presents the damper characterization data. In this study, aisle C had nine dampers and nine perforated tiles with a fixed opening. The ITE airflow demand in aisle C was equal to 9898 CFM (Table 1). Based on the results in Fig. 6a, considering  $\Delta P = 5Pa$  across the dampers, 736 CFM airflow was obtained from each damper. The remaining amount of flow rate, which was 3274 CFM, was expected to be supplied from the perforated tiles. A plenum pressure of 5 Pa satisfied this expectation. To be in a safe zone, 6 Pa was considered as the lower bound of plenum pressure.

The upper bound of plenum pressure was specified by conducting a simple experiment. The experiment started when all the dampers were completely opened in both aisles C and D. At every stage, the  $\Delta P$  across the CAC and the airflow rate of the perforated tiles were measured. Gradually, the damper openness in aisle C was decreased by 20%, while in aisle D the dampers remained unchanged. By decreasing the OAR of the dampers in one aisle, the CAC pressure in the other aisle and plenum pressure was increased because both aisles had a common plenum. Fig. 6b depicts the positive correlation of pressure and leakages in the RF plenum. The nominal flow rate of CRAH 1 and 2 reported by the manufacturer was 17 300 CFM and 16 500 CFM, respectively. Considering 7% of leakages in the DC laboratory (2366 CFM), the pressure in the plenum was less than 11 Pa, which established the upper range of plenum pressure.

### 3.4. Developing an artificial neural network for damper characterization

Precise experimental measurements were conducted in the previous section to characterize the air dampers for different OAR and the ΔP across the dampers. As shown in Fig. 6a, the nature of the system was complicated and nonlinear. To estimate the required range of plenum pressure in any DC regardless of RF dimension, the airflow rate for each dampers' openness or the ΔP across the dampers needs to be captured. It is challenging and time consuming to implement this approach experimentally. As a result, an ANN, which is a nonlinear regression tool (Srikanth & Balaji, 2017), was developed using MATLAB. One of the advantages of adopting an ANN is its efficiency in handling nonlinear trends in DC compared to a conventional polynomial expression. Furthermore, the neural network based regression helps future system optimization. A supervised learning (Srikanth, Nemani, & Balaji, 2015) based static ANN was employed in this study. The ANN development procedure was as follows:

(a) The dampers' OAR and differential pressure across the dampers were considered as the input layers while the acquired airflow from dampers was employed as the output layer.(b) The available data collected from the experiments was divided into three groups, namely training, validation, and testing data sets. In total, 187 sets of data collected from the experiments provided input for the network. 89% of data sets were allocated to the training, 11% of which were employed to evaluate the network. Twenty one sets of data within the limits of the variables were considered for testing the robustness of the network. (c)

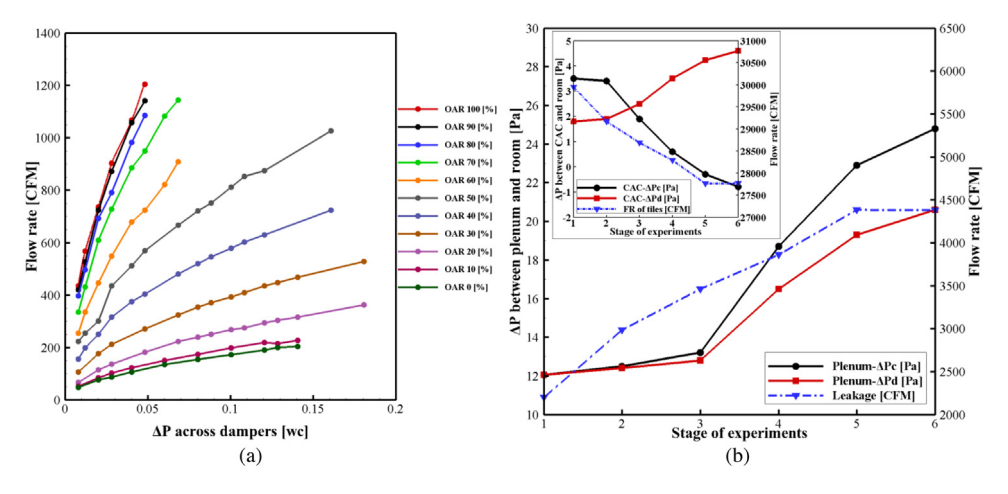


Fig. 6. (a) Damper characterization data. (b) DC leakage estimation based on the plenum pressure.

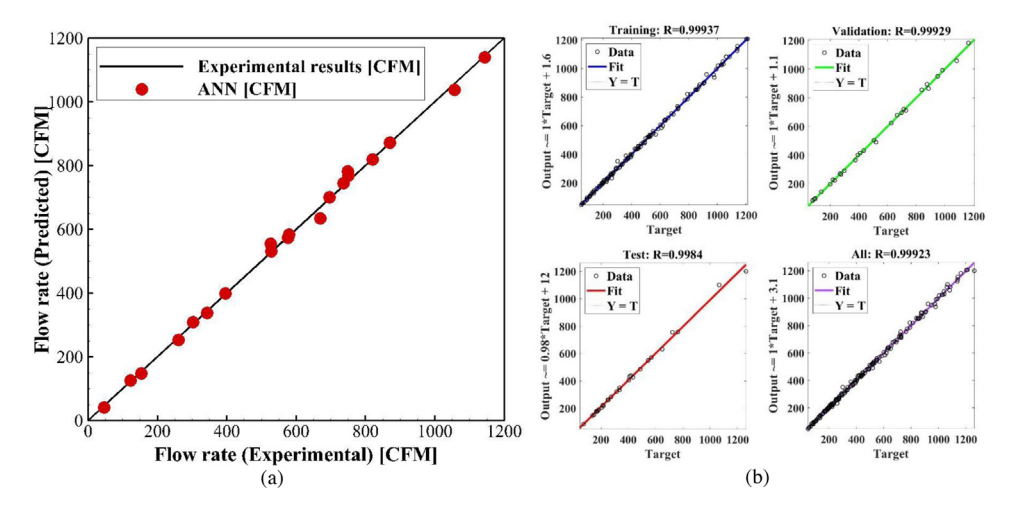


Fig. 7. (a) Parity plot. (b) Training, test, and validation data sets.

The data was normalized in the range of [-1, 1] as the tan hyperbolic function had its limiting values in the range [-1, 1]. (d) The optimal number of neurons was determined using the neuron independent study. In this study, the optimal number of neurons was calculated to be 24.

The result of the regression analysis is shown in Fig. 7. The network's prediction had a good agreement with the actual experimental data for different OAR and differential pressure across the dampers. The Parity plot obtained from the ANN made it evident that the curve fitting was accurate for this nonlinear problem. This can be attributed to the regressive sensitivity analysis performed during the training process of the ANN. The ANN simplified the complex problem using an effective surrogate model. The surrogate model can be used for further data analysis.

### 4. Results and discussion

### 4.1. Scenario I

This scenario aimed to demonstrate the performance of dampers' fuzzy controller in the presence of ITE load variation for two aisles (C & D) simultaneously. Fig. 8a and b illustrate  $\Delta P_{\text{CAC-room}}$  and  $\Delta P_{\text{Plenum-room}}$  versus the control system response time, respectively. Approximately 80% of all the servers in aisle C were initially turned off (racks C1–1 to C1–6 and C2–1 to C2–6) and then on to mimic variation in the ITE airflow demand. At the same time, servers in aisle D ran in idle mode for the duration of the experiment. Initially, all dampers

in aisles C and D were completely opened and the aisles were over provisioned. As a result, the control system decreased the dampers' OAR and tried to reach zero  $\Delta P$  across the aisles. The transient response time of the system was 15.9 min. However, as shown in Fig. 8a, aisle C remained over provisioned by ~2 Pa even when the dampers' OAR in aisle C were 0% (t = 15 min). Moreover, closing all the dampers increased the plenum pressure to 40 Pa and hence enlarged the plenum leakages. Given this, it was necessary to control the cold air delivery from the cooling units to the individual aisles, which will be discussed in Section 4.2. The system stayed in sleep mode for approximately 27 min to ensure a steady state was reached. At t = 42 min, all 12 racks of servers in aisle C were turned back on to mimic an increase in the ITE load. Consequently, the pressure dropped to −6 Pa and −0.34 Pa in aisles C and D, respectively. The controller responded by increasing the dampers' OAR, which brought the CAC pressure within the ideal range  $(0 < \Delta P < 1)$  after 12.7 min. It is worth mentioning that the pressure variation inside the CAC and the plenum for aisle D occurred due to the increasing and decreasing ITE load in aisle C.

### 4.2. Scenario II (COLO data center)

In this experiment, two different thermal zones were considered, and a colocation DC was introduced. The performance of the two fuzzy controllers in series was tested in over provisioned aisles. The CRAH units' SATs were set to be 22 °C. At the initial state of the experiment, all dampers were completely open and the CRAHs' blower speeds were maximum. Both aisles C and D were over provisioned. The damper

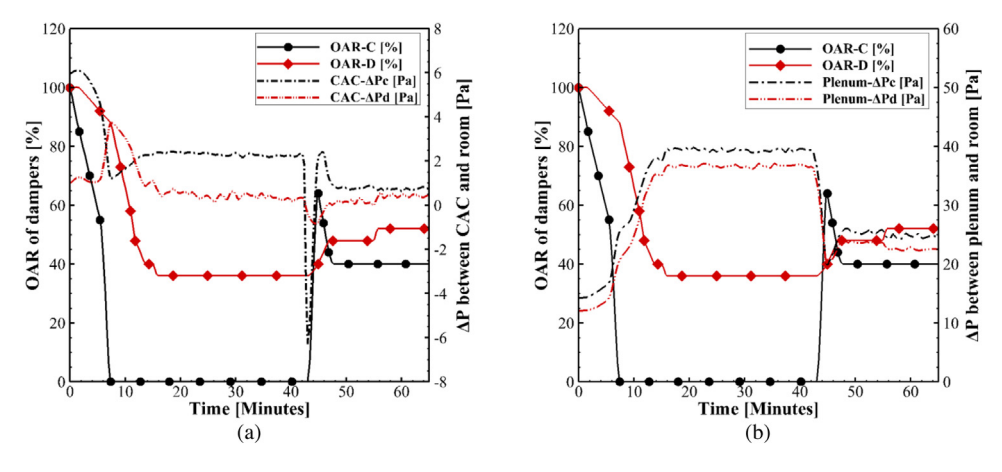


Fig. 8. (a) Dampers' OAR vs. CAC differential pressure. (b) Dampers' OAR vs. plenum differential pressure.

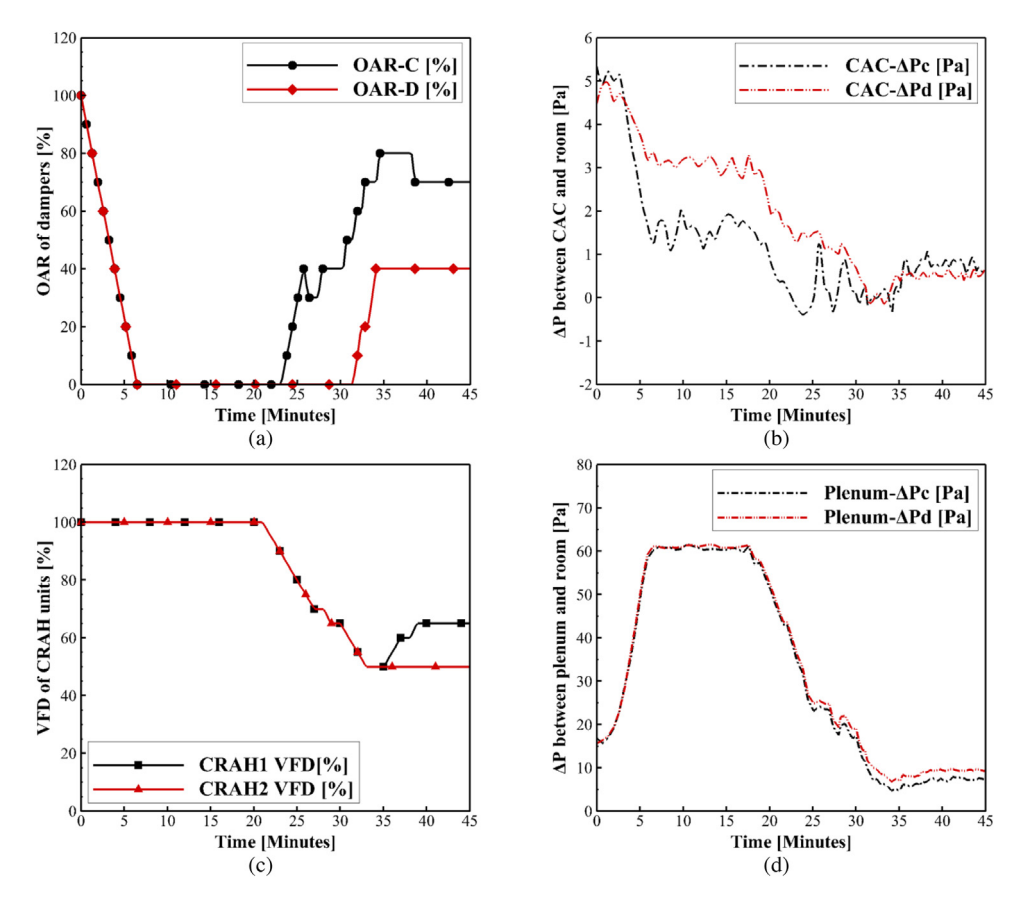


Fig. 9. Results of experiment in scenario II. (a) Dampers' OAR. (b) CAC differential pressure. (c) VFD of cooling units. (d) Plenum differential pressure.

controller was run first, which sent a signal to decrease the dampers' openness, resulting in CAC pressure reduction. Despite the dampers' OAR of 0%, aisles C and D remained over provisioned (Fig. 9a and b). The transient response time of the system was 7 min. It is noteworthy that reducing the dampers' openness increased the plenum pressure to 60 Pa, which increased plenum leakages. The system was in sleep mode for about 20 min to ensure a steady state. At t=21 min, the cooling units' blower speeds control system was run to regulate the pressure in the RF if needed. The CRAH1's blower speed was controlled by the average pressure under aisle C. The controlled variable for the VFD of CRAH2 was the plenum pressure under aisle D. Fig. 9c and d demonstrate the CRAH units' VFD and plenum pressure for aisles C and D versus the control system response time, respectively. The fuzzy feedback controller decreased the cooling units' VFD to

generate the required range of plenum pressure (6 Pa <  $\Delta P_{Required}$  < 11 Pa). By decreasing the VFD of the CRAH units, CAC pressure was consequently reduced. Therefore, the dampers' OAR was increased to maintain neutral pressure in CAC. It took approximately 40 min for the system to reach the desired provisioning state inside CAC and the specified range of pressure in the RF plenum. It is worth mentioning that the maximum inlet air temperature of the servers in aisles C and D obtained from IPMI data and external temperature sensors was 23 °C throughout the experiments. Although the cooling units' blower speeds and dampers' OAR decreased from their initial set points, the servers' inlet temperatures stayed constant using the proposed control methodology, which improved the DC energy efficiency.

The effect of these two controllers on the tiles flow rate is shown in Table 2. The difference between the measured tiles' flow deliveries via

a flow hood and the estimated airflow demand of the ITE is presented in the "Difference" row. Regulating the fan speeds of the cooling units along with the openness of the air dampers caused a 72% reduction in the level of over provisioning in aisles C and D.

### 4.3. Scenario III

In this scenario, the performance of the damper controller and the cooling units' blower speeds control system were studied for under provisioned aisles. The number of perforated tiles inside aisles C and D was reduced by 50% since perforated tiles were substituted with solid tiles within the aisles. There were only nine and ten dampers in aisles C

 Table 2

 Percentage of over provisioning of aisles C and D during different stages in scenario II.

	Initial steady state	Final steady state
Tiles' flow rate	32 365 cfm	19115 cfm
Estimated flow rate demand	18534 cfm	18534 cfm
Difference	13 831 cfm	581 cfm
% Over provisioning	75%	3%

and D, respectively (Fig. 4e). The dampers were completely closed and both aisles C and D were under provisioned at the initial state. First,

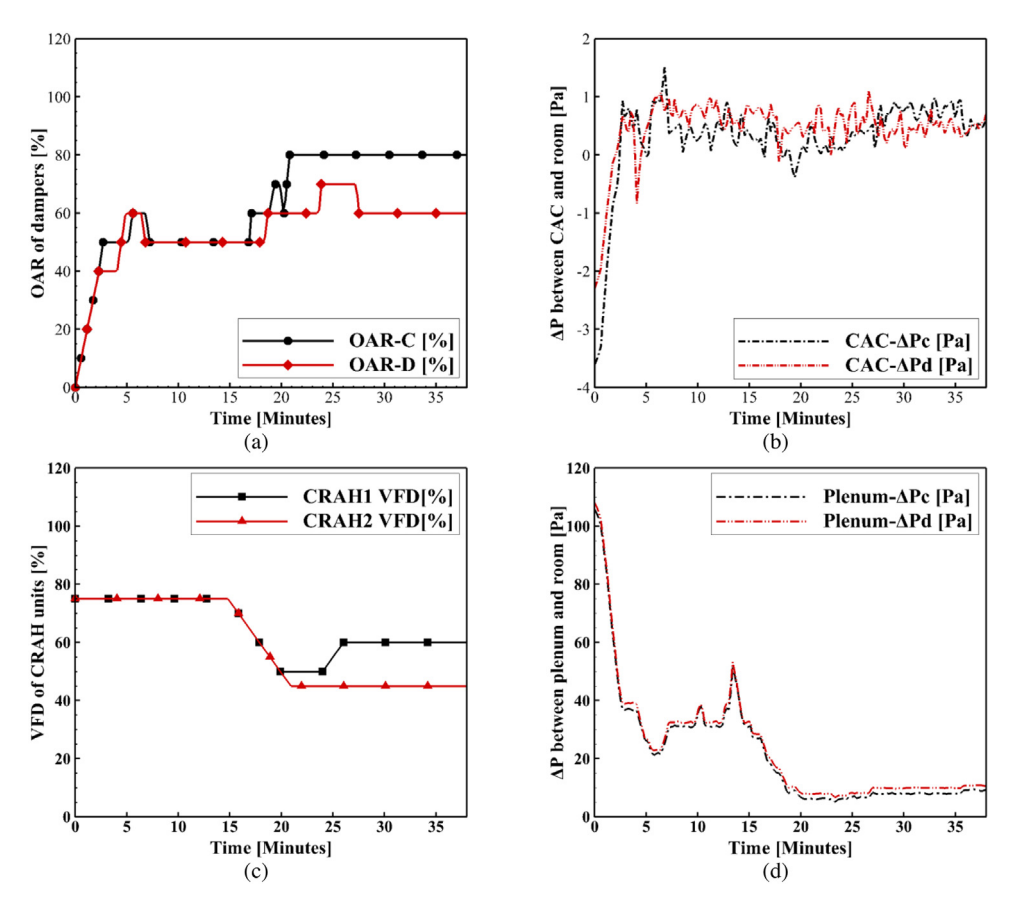


Fig. 10. Results of experiment in scenario III. (a) Dampers' OAR. (b) CAC differential pressure. (c) VFD of cooling units. (d) Plenum differential pressure.

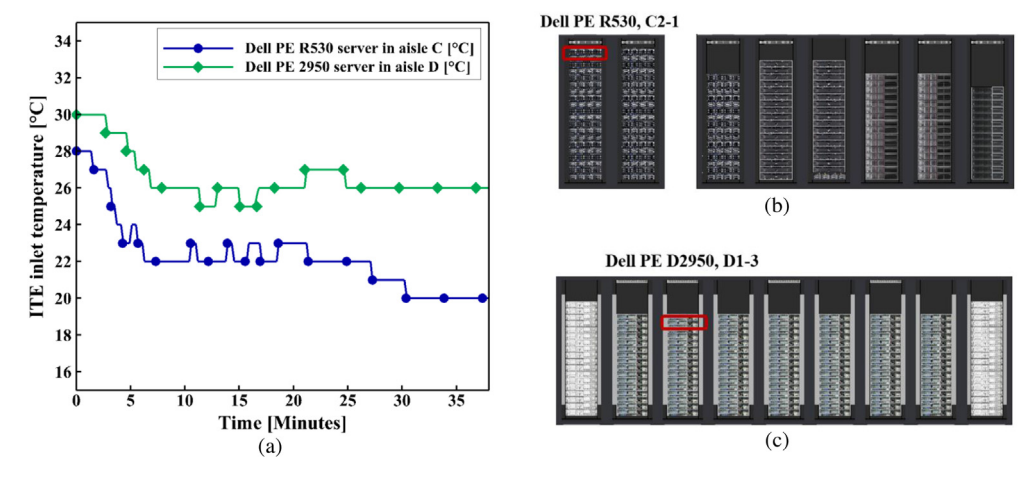


Fig. 11. (a) IPMI maximum inlet temperature data for two servers in aisle C and D. (b) Location of Dell PE R530 server in aisle C. (c) Location of Dell PE D2950 server in aisle D

the damper controller compensated for the negative pressure inside CAC by increasing the dampers' OAR, as seen in Fig. 10a and b. The system rested between 7.2 min < t < 15 min to ensure a steady state. Meanwhile, the plenum pressure was above the desired upper range. As a result, at t = 15 min, the CRAH VFD control system decreased the blower speed to lower the RF pressure (Fig. 10c and d). After 27.5 min, the automated system attained the desired conditions, which were neutral pressure inside the CAC and a plenum pressure between 6 Pa and 11 Pa. Although the number of perforated tiles was decreased by 50%, both aisles C and D reached the desired provisioning level using the proposed control scheme.

Furthermore, the servers' inlet temperatures were obtained by gathering IPMI data in this experiment. Fig. 11a represents the maximum ITE inlet temperature for Dell PE R530 in aisle C and Dell PE d2950 in aisle D. The inlet temperatures of all other servers in aisles C and D were less than these two servers. As represented in Fig. 11b and c, both servers were located at the top of the racks. The directional tiles installed in aisles C and D directed the airflow to the racks' faces. As a result, the pressure at the inlet of severs was higher at lower elevations where the servers were closer to the tiles. Moreover, the air temperature increased at higher elevations within the facility. Hence, there was a higher probability that the ITE at the top of the racks would get overheated. At the early stages of the experiment, the lack of cold air caused negative pressure inside the aisles. Thus, the servers' inlet temperatures increased to 28 °C and 30 °C in aisles C and D, respectively. After running the two fuzzy controllers, the aisles reached the desired provisioning state and the ITE inlet temperature decreased to the allowable temperature range specified by the ASHRAE recommended guidelines (ASHRAE Technical Committee 9.9, 2015).

### 4.4. Thermal images

To determine the temperature map, potential leak path, and hot spots inside the cold aisles for different conditions (under provisioning, provisioning, and over provisioning), thermal images were taken via an infrared (IR) camera (Fig. 12). Although the IR camera showed the surface temperature of the objects, it was assumed that the surface temperature represented the airflow temperature passing over them in a steady state. As a result, an adequate amount of time was allocated for the system to reach a steady state in each condition.

As expected, in an over provisioned state, the surface temperature was 20 °C and equal to the SAT from the cooling units. In a fully provisioned state, aisle D had a slightly higher temperature and more hot spots than aisle C, especially near the end of the aisle. Some of the servers at the end of aisle D were turned off, indicating red spots on the thermal image. Furthermore, the higher temperature at the top of the racks in aisle D was attributed to the exposure of blanking panels and hot air in the hot aisle. Another explanation was that the blade center servers in the D2 rows consumed more airflow than the Dell 2950 servers on the other side of aisle D. Subsequently, the servers on the left-hand side of aisle D struggled for an adequate amount of cold air. It is notable that in a fully provisioned state, all the ITE in aisles C and D were within the allowable temperature range specified by the ASHRAE guidelines (ASHRAE Technical Committee 9.9, 2015). However, in an under provisioned state, both aisles C and D had noticeable hot spots, recirculation, and leaks.

### 5. Energy saving evaluation

### 5.1. Cooling units' fan savings

A major part of power consumption in a DC space is used to drive out heat generated by the ITE, particularly by the CRAH units' fans and the chiller plant. Therefore, the power consumption and energy savings for the CRAH units' fans and chiller plant from scenario II in Section 4.2 were investigated. Based on the tiles' flow rates data in Table 2, by implementing two controllers, the airflow delivery to aisles C and D were decreased by 40%. According to fan laws (Bleier, 1998), shown in Eq. (1), a 40% reduction in flow rate will reduce the blower power by 80%. The law assumes that the fan efficiency remains constant, which is rarely true in practice. Moreover, because of air bypasses through the RF gaps, the actual power saved was expected to be less than 80%.

$$\frac{P_2}{P_1} = \left(\frac{Q_2}{Q_1}\right)^3 \tag{1}$$

In scenario II, based on the airflow demand of ITE in aisles C and D, the fuzzy controller reduced the CRAH units' blower speeds by 35% and 50% for CRAHs 1 and 2, respectively. This reduction in fan speed led to lower power consumption and a 75% savings in energy (Table 3).

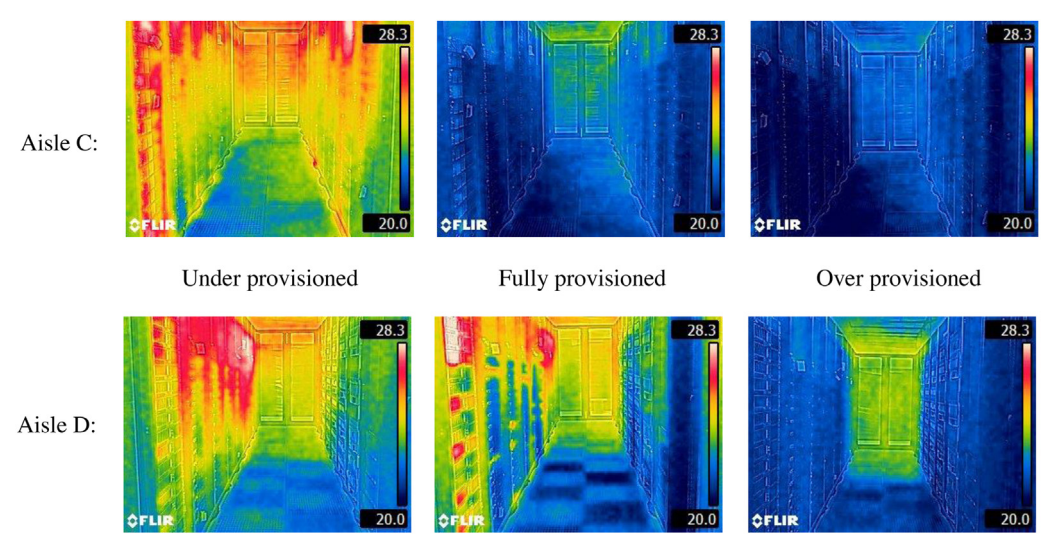
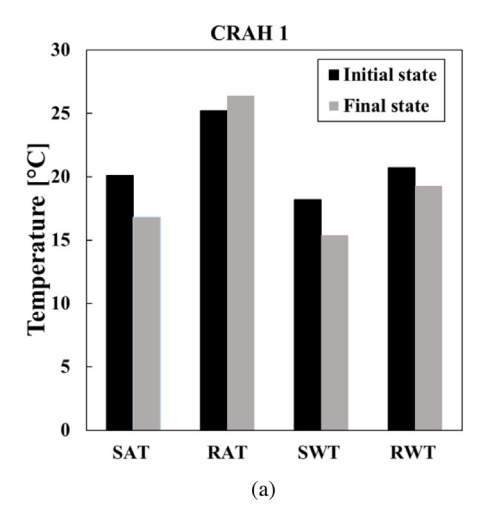


Fig. 12. Thermal images of aisles C & D under different conditions.



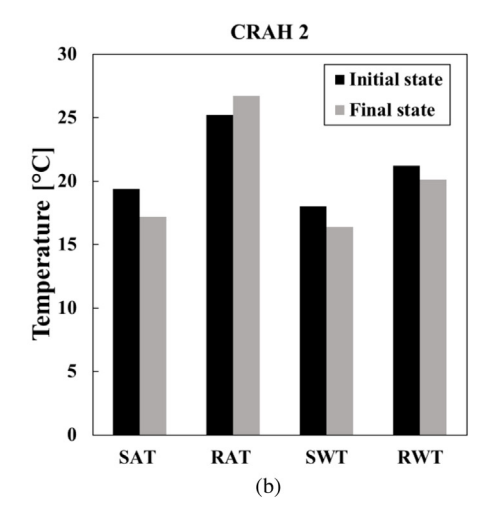


Fig. 13. Supply Air Temperature (SAT), Return Air Temperature (RAT), Supply Water Temperature (SWT), and Return Water Temperature (RWT) of cooling units during the experiments in scenario II. (a) Corresponding data for CRAH 1. (b) Corresponding data for CRAH 2.

Table 3
Cooling units' blower saving in scenario II.

	. 0			
States	VFD of	Power of	VFD of	Power of
	CRAH1 (%)	CRAH1 (kW)	CRAH2 (%)	CRAH 2 (kW)
Initial steady state	100	9.5	100	9.1
Final steady state	65	2.6	50	2
Power saving	14 kW			

### 5.2. Chiller plant saving

There was another potential energy saving opportunity for the chiller plant through the dynamic airflow management technique. The building's chilled water was used for either the ES2 data center cooling or to air condition other laboratories in the building. Since the ES2 data center did not have its own dedicated chiller, a direct calculation of energy savings in the chiller plant was not possible. Considering this, an experiment was designed to estimate the potential chiller savings in scenario II. First, the two fuzzy controllers were run. Then, the cooling units' blower speeds were lowered to supply adequate air to the ITE environment. Afterward, the amount of chilled water flowing from the building's chiller to the CRAHs was decreased manually by decreasing the pump speed. Fig. 13 shows that despite the total heat dissipated by the ITE remaining constant during the test, the overall temperature growth was higher in the final steady state. This is noteworthy because a higher rack air temperature difference across the ITE and a higher temperature difference of the chiller fluids will lead to a more efficient heat transfer in the CRAH coils. In turn, this improves the chiller's overall cooling performance. The results showed a 16% savings in chiller power consumption (Table 4). It is worth mentioning that enough time was allocated for the system to achieve a steady state. Overall, the total power saved for the ES2 data center in this scenario was approximately 30 kW. By implementing the proposed control scheme in a DC with only two cooling units, \$52,560 can potentially be saved annually with an assumption of \$0.2 per kWh of electricity.

### 6. Concluding remarks

In this paper, a holistic DC cooling control approach was examined based on the  $\Delta P_{\text{CAC-room}}$  and  $\Delta P_{\text{Plenum-room}}$  to optimize aisles provisioning and the distribution of cooling resources. Within many DCs, the complexity of managing airflow while making continuous adjustments makes using an automatic control system necessary. Cooling approaches that use a fixed CRAH blower speed and fixed tile perforation provide no local flexibility in how cold air is delivered to ITE racks and no local feedback information on the state of airflow for different areas of a DC. While these methods often require less hardware, they are inefficient and not readily adaptable to changes in the environment. Without flexibility, there is little potential to optimize DC operation. Therefore, to efficiently manage the cold air delivered to individual aisles, it is essential to control the openness of dampers and the cooling units' fan speeds. The two fuzzy controllers developed for this study operated independent of the model, generation, number and workload of installed ITE, and layout of server racks and cooling units in the DC. Working in series, the two controllers successfully ensured adequate provisioning of the servers under different circumstances and with ITE load variation. One challenge was implementing the proposed control scheme in multiple aisles that were connected through a common plenum. To overcome this challenge, different time constants were allocated for the two controllers. Another critical obstacle was estimating the required range of pressure in the plenum. Regarding this, the developed neural network provided an estimation of the required range of plenum pressure regardless of the RF dimensions. Using the neural network can also facilitate future system optimization. The proposed cooling control strategy has been shown to save 75% of the cooling units' blower powers and 16% of the chiller power. The authors are working on testing the proposed cooling control strategy in a large-scale DC using the validated numerical model to extend the work presented. For future studies, the sequence of running the controllers that can affect the system's total response time can be investigated.

Table 4 Cooling units' chiller saving in scenario II.

	States	m <sub>water</sub> (kg/s)	RWT- SWT (°C)	Q (kW)		States	m <sub>water</sub> (kg/s)	RWT- SWT (°C)	Q (kW)
CRAH 1	Initial S.S.	4.3	2.5	44.7	CRAH2	Initial S.S.	4.1	3.2	54.8
	Final S.S.	2.5	3.9	40.8		Final S.S.	2.7	3.7	42.7
Power saving					16	kW			

### CRediT authorship contribution statement

Ghazal Mohsenian: Conceptualization, Methodology, Designing control strategy algorithm, Building the experimental apparatus, Conducting experiments, Formal analysis, Validation, Software, Writing-original draft, Writing-review & editing. Sadegh Khalili: Methodology, Building the experimental apparatus, Review. Mohammad Tradat: Methodology, Building the experimental apparatus, Review. Yaman Manaserh: Methodology, Building the experimental apparatus, Review. Srikanth Rangarajan: Methodology, Review. Anuroop Desu: Optimization and debugging the bash script of the control system. Dushyant Thakur: Optimization and debugging the bash script of the control system. Kourosh Nemati: Supervision, Funding acquisition, Methodology. Kanad Ghose: Supervision, Funding acquisition, Methodology. Bahgat Sammakia: Supervision, Funding acquisition, Methodology.

### Declaration of competing interest

The authors declare that they have no known competing financial interests or personal relationships that could have appeared to influence the work reported in this paper.

### Acknowledgments

The authors would like to acknowledge Mark Seymour from Future Facilities, Tod Schreiber from Bloomberg, and Russ Tipton and Arash Golafshan from Vertiv for their support and advice. This work is supported by NSF IUCRC, United States of America Award No. IIP-1738793 and MRI, United States of America Award No. CNS1040666.

### References

- Alissa, Husam A., et al. (2016a). Chip to chiller experimental cooling failure analysis of data centers: The interaction between IT and facility. In *IEEE Transactions on Components, Packaging and Manufacturing Technology, Vol. 6* (9), (pp. 1361–1378). IEEE.
- Alissa, H. A., et al. (2016b). Chip to facility ramifications of containment solution on IT airflow and uptime. IEEE Transactions on Components, Packaging and Manufacturing Technology, 6(1), 67–78. http://dx.doi.org/10.1109/TCPMT.2015.2508453.
- Arghode, V. K., Sundaralingam, V., & Joshi, Y. (2016). Airflow management in a contained cold aisle using active fan tiles for energy efficient data-center operation. Heat Transfer Engineering, 37(3-4), 246-256. http://dx.doi.org/10.1080/01457632. 2015.1051386, Taylor & Francis.
- ASHRAE Technical Committee 9. 9 (2015). Thermal Guidelines for Data Processing Environments (fourth ed.). Atlanta: W. Stephen Comstock.
- Athavale, J., Joshi, Y., & Yoda, M. (2018). Experimentally validated computational fluid dynamics model for data center with active tiles. *Journal of Electronic Packaging.* American Society of Mechanical Engineers, 140(1), 10902.
- Bash, C. B., Patel, C. D., & Sharma, R. K. (2006). Dynamic thermal management of air cooled data centers. In *Thermal and Thermomechanical Proceedings 10th Intersociety Conference on Phenomena in Electronics Systems* (p. 8). ITHERM 2006, http://dx.doi.org/10.1109/ITHERM.2006.1645377, - 452.
- Baxendale, M., et al. (2019). Data center temperature control using PI system and MAT-LAB. In 2019 18th IEEE Intersociety Conference on Thermal and Thermomechanical Phenomena in Electronic Systems (ITherm) (pp. 897–904). IEEE.
- Beitelmal, M. H., et al. (2009). Local cooling control of data centers with adaptive vent tiles. In ASME 2009 InterPACK Conference Collocated with the ASME 2009 Summer Heat Transfer Conference and the ASME 2009 3rd International Conference on Energy Sustainability (pp. 645–652). American Society of Mechanical Engineers Digital Collection.
- Bleier, F. P. (1998). Fan Handbook. McGraw-Hill New York.
- Boucher, T. D., et al. (2005). Viability of dynamic cooling control in a data center environment. *Journal of Electronic Packaging*, 128(2), 137–144. http://dx.doi.org/ 10.1115/1.2165214, ASME, Available at:.
- Chu, W.-X., & Wang, C.-C. (2019). A review on airflow management in data centers. Applied Energy, 240, 84–119, Elsevier.
- Garcia-Gabin, W., Mishchenko, K., & Berglund, E. (2018). Cooling control of data centers using linear quadratic regulators. In 2018 26th Mediterranean Conference on Control and Automation (MED) (pp. 1–6). http://dx.doi.org/10.1109/MED.2018. 8442429.
- Ham, S.-W. others (2015). Energy saving potential of various air-side economizers in a modular data center. Applied Energy, 138, 258–275, Elsevier.

- Khalid, R., & Wemhoff, A. P. (2019). Thermal control strategies for reliable and energy-efficient data centers. *Journal of Electronic Packaging*, 141(4), American Society of Mechanical Engineers Digital Collection.
- Khalili, S., et al. (2018). Impact of tile design on the thermal performance of open and enclosed aisles. *Journal of Electronic Packaging*, *140*(1), 10907–10912. http://dx.doi.org/10.1115/1.4039028, ASME, Available at:.
- Khalili, S., et al. (2019). Airflow management using active air dampers in presence of a dynamic workload in data centers. In 35th Annual Semiconductor Thermal Measurement, Modeling and Management Symposium, SEMI-THERM 2019 Proceedings.
- Klir, G., & Yuan, B. (1995). Fuzzy Sets and Fuzzy Logic. Prentice hall New Jersey. Lucchese, R., & Johansson, A. (2019). On energy efficient flow provisioning in air-cooled data servers. Control Engineering Practice, 89, 103–112, Elsevier.
- Manaserh, Y. M., Tradat, M. I., Mohsenian, G., Sammakia, B. G., Ortega, A., et al. (2020). Novel experimental methodology for characterizing fan performance in highly resistive environments. In 2020 19th IEEE Intersociety Conference on Thermal and Thermomechanical Phenomena in Electronic Systems (ITherm) (pp. 1–7). http://dx.doi.org/10.1109/ITherm45881.2020.9190308.
- Manaserh, Y. M., Tradat, M. I., Mohsenian, G., Sammakia, B. G., & Seymour, M. J. (2020). General guidelines for commercialization a small-scale in-row cooled data center: A case study. In 2020 36th Semiconductor Thermal Measurement, Modeling & Management Symposium (SEMI-THERM) (pp. 48–55). http://dx.doi.org/10.23919/SEMI-THERM50369.2020.9142847.
- Mohsenian, G. (2020). A Novel Integrated Fuzzy Control System Towards Automated Local Airflow Management in Data Centers (ProQuest Dissertations and Theses), State University of New York at Binghamton, Available at: http://proxy.binghamton.edu/login? https://www.proquest.com/dissertations-theses/novel-integrated-fuzzy-control-system-towards/docview/2449439443/se-2?.
- Mohsenian, G., Khalili, S., & Sammakia, B. (2019). A design methodology for controlling local airflow delivery in data centers using air dampers. In 2019 18th IEEE Intersociety Conference on Thermal and Thermomechanical Phenomena in Electronic Systems (ITherm) (pp. 905–911). IEEE.
- Muralidharan, B., et al. (2013). Impact of cold aisle containment on thermal performance of data center. http://dx.doi.org/10.1115/IPACK2013-73201, V002T09A016, Available at:.
- Nada, S. A., & Said, M. A. (2017). Comprehensive study on the effects of plenum depths on air flow and thermal managements in data centers. *International Journal* of Thermal Sciences, 122, 302–312, Elsevier.
- Nada, S. A., et al. (2017). Experimental parametric study of servers cooling management in data centers buildings. *Heat and Mass Transfer*, 53(6), 2083–2097, Springer.
- Nemati, K. others (2016). Steady-state and transient comparison of cold and hot aisle containment and chimney. In 2016 15th IEEE Intersociety Conference on Thermal and Thermomechanical Phenomena in Electronic Systems (ITherm) (pp. 1435–1443). http://dx.doi.org/10.1109/ITHERM.2016.7517717.
- Nemati, K., Alissa, H., & Sammakia, B. (2015). Performance of temperature controlled perimeter and row-based cooling systems in open and containment environment. In ASME 2015 International Mechanical Engineering Congress and Exposition. American Society of Mechanical Engineers Digital Collection.
- Raymond, C., Boverie, S., & Titli, A. (1994). First evaluation of fuzzy MIMO control laws. In Proceedings of 1994 IEEE 3rd International Fuzzy Systems Conference (pp. 545–548). IEEE.
- Rong, H., et al. (2016). Optimizing energy consumption for data centers. Renewable & Sustainable Energy Reviews, 58, 674–691, Elsevier.
- Saiyad, A., et al. (2021). Predictive modeling of thermal parameters inside the raised floor plenum data center using artificial neural networks. *Journal of Building Engineering*, 42, Article 102397. http://dx.doi.org/10.1016/j.jobe.2021.102397.
- Shrivastava, S. K., Calder, A. R., & Ibrahim, M. (2012). Quantitative comparison of air containment systems. In 13th InterSociety Conference on Thermal and Thermomechanical Phenomena in Electronic Systems (pp. 68–77). IEEE.
- Shrivastava, S. K., & Ibrahim, M. (2013). Benefit of cold aisle containment during cooling failure. http://dx.doi.org/10.1115/IPACK2013-73219, V002T09A021. Available at:.
- Simoes, M. G. (2010). Introduction to fuzzy control, Vol. 8 (pp. 18–22). Colorado School of Mines, Engineering Division, Golden, Colorado.
- Song, Z., Murray, B. T., & Sammakia, B. (2013). Airflow and temperature distribution optimization in data centers using artificial neural networks. *International Journal* of Heat and Mass Transfer, 64, 80–90, Elsevier.
- Song, Z., Murray, B. T., & Sammakia, B. (2014). A dynamic compact thermal model for data center analysis and control using the zonal method and artificial neural networks. *Applied Thermal Engineering*, 62(1), 48–57. http://dx.doi.org/10.1016/j. applthermaleng.2013.09.006.
- Srikanth, R., & Balaji, C. (2017). Experimental investigation on the heat transfer performance of a PCM based pin fin heat sink with discrete heating. *International Journal of Thermal Sciences*, 111, 188–203. Elsevier.
- Srikanth, R., Nemani, P., & Balaji, C. (2015). Multi-objective geometric optimization of a PCM based matrix type composite heat sink. Applied Energy, 156, 703-714, Elegitor.
- Tradat, M., et al. (2020). Experimental analysis of different measurement techniques of server-rack airflow predictions towards proper DC airflow management. In 2020 19th IEEE Intersociety Conference on Thermal and Thermomechanical Phenomena in Electronic Systems (ITherm) (pp. 366–373). http://dx.doi.org/10.1109/ ITherm45881.2020.9190584.

- Wang, C.-H., Tsui, Y.-Y., & Wang, C.-C. (2017). Airflow management on the efficiency index of a container data center having overhead air supply. *Journal of Electronic Packaging*, 139(4), 41008, American Society of Mechanical Engineers.
- Wang, Z., et al. (2009). Kratos: Automated management of cooling capacity in data centers with adaptive vent tiles. (pp. 269–278). http://dx.doi.org/10.1115/ IMECE2009-11747.
- Wong, C.-C., & Feng, S.-M. (1994). A switching type of fuzzy controller. In Proceedings of 1994 IEEE 3rd International Fuzzy Systems Conference (pp. 30–34). IEEE.
- Zadeh, L. A. (1973). Outline of a new approach to the analysis of complex systems and decision processes. *IEEE Transactions on Systems, Man, and Cybernetics*, SMC-3(1), 28–44. http://dx.doi.org/10.1109/TSMC.1973.5408575.
- Zheng, Q., et al. (2018). An optimized active disturbance rejection approach to fan control in server. *Control Engineering Practice*, 79, 154–169, Elsevier.